

Recent knowledge about the role of bacterial adhesion in coal preparation

Jiří Škvarla¹, Daniel Kupka² and Ľudmila Turčániová²

Súčasný poznatky o úlohe adhézie baktérií v úprave uhlia

V nadväznosti na flotáciu pyritu v uhlí sú zhrnuté súčasné poznatky o vplyve fyzikálno-chemických vlastností bunečnej steny baktérie *Thiobacillus ferrooxidans* na jej adhéziu na povrch rôznych minerálov a uhlia. Aplikovaním modelu mikrobiálnej adhézie (Škvarla, J. *Chem. Soc. Faraday Trans.*, 89, 1993, p. 2913-2921) a využitím známych parametrov vstupujúcich do tohoto modelu bolo zistené, že k (reverzibilnej) adhézii *T. ferrooxidans* dochádza spravidla v sekundárnom minime. Pre posúdenie možnosti využitia tohoto modelu na objasnenie selektívneho prichytenia *T. ferrooxidans* na pyrit je však potrebné doplniť chýbajúce údaje vstupujúce do tohoto modelu.

Key words: microbial adhesion, surface properties, *Thiobacillus ferrooxidans*.

Introduction

Microbial flotation is the technology of choice among the microbial desulfurization methods, as it can remove pyritic sulfur faster than the leaching method. It has been found that the suppression of pyrite is caused by the selective adhesion of *T. ferrooxidans* on its surface (Ohmura and Saiki, 1994, 1996; Attia et al., 1993). That is why the process of the microbial adhesion on mineral surfaces itself is of prime importance. In the paper, a present knowledge about this phenomenon has been summarized in order to evaluate the general physico-chemical model of microbial adhesion proposed earlier by one of us (Škvarla, 1993). Both the bacterial cell wall and the mineral surface characteristics, involved in the model, have been considered.

Bacterial cell wall surface characteristics

In order to gain information about chemical and biochemical events at the mineral surface during its dissolution in the presence of sessile (adhered) and planktonic (free) bacteria, Blake II et al. (1994) used the electrophoretic light scattering (ELS) spectra (by the laser Doppler velocimetry) for evaluating the interaction of the *T. ferrooxidans* ATCC 23270 cells with ferric ions, colloidal pyrite and sulfur at its physiological conditions (pH 2). It has been found that:

(1) *T. ferrooxidans* grown on soluble ferrous ions (with the product ferric ions being electrochemically reduced 1 h prior to harvesting) and resuspended (10^8 cells/ml) in 10^{-2} N solutions of sulfuric, perchloric, hydrochloric, or nitric acid had the reproducible value of zeta potential (ζ) -6.0, -7.4, -4.7, and -1.8 mV, respectively. After addition of ferric ions (as salts of the corresponding conjugate base so that each solution contained only one major species of anion) the above values were lowered (less negative) according to a rectangular hyperbolic function. For example, at concentration of Fe(III) perchlorate 25 mM (the upper limit concentration) was $\zeta \approx 0$. Evidently, Fe (III) ions were preferentially adsorbed to *T. ferrooxidans*. Interestingly, ζ -potential of cells grown to stationary phase on soluble ferrous ions and harvested from an environment high in ferric ions (i.e. under oxidizing conditions) varied from culture to culture ranging from -5.0 to +1.5 mV. Efforts to devise a washing routine were unsuccessful. AAS analyses on the whole-cell lysates revealed that such cells had even sevenfold more iron associated with them than did cells harvested in the presence only ferrous ions under reductive conditions (1.0×10^{-12} g Fe/cell vs. 1.4×10^{-13} g Fe/cell, respectively).

¹ Department of Mineral Processing and Environmental Protection, Technical University, Park Komenského 19, 04384 Košice

² Institute of Geotechnics, Slovak Academy of Sciences, Watsonova 45, 04353 Košice, Slovak Republic

(Received July 20, 1998)

(2) The ζ -potential of *T. ferrooxidans* was also influenced by its growth history. It was more negative for cells cultured on (only) ferrous ions (-7.4 mV in 10^{-2} N perchloric acid) than for cells cultured on pyrite (-2.2 mV) or on the elemental sublimed sulfur (-0.1 mV). In both latter cases, the substrate associated cells were recovered by 10^{-2} % (wt/vol) Triton X-100 and washed three times with 10^{-3} N sulfuric acid. The less negative values of ζ for the pyrite-grown cells relative to those in ferrous ions-grown cells could be due to the residual ferric ions present in their cell wall (8.0×10^{-13} g/cell). The binding patterns obtained by gell electrophoresis, determining the number and nature of outer membrane and cell wall components, revealed that the growth history had also an influence on the structure of the cells outside.

(3) Based on the linear dependence of the peak half-width at half-height versus the sine of the bisected scattering angle, a heterogeneity in the electrophoretic mobility of the cells population was the major source of broadening of the ELS spectra obtained for *T. ferrooxidans*. In contrast, the ELS spectra obtained for unfractionated pyrite (autoclaved as the dry powder, reduced by amalgamation, grinded with a mortar and pestle, suspended in distilled water, and separated by decantation as the fraction of particles remaining dispersed after 2 h of sedimentation) were not only complex (multimodal), reflecting the polydispersity of the pyrite particles, but broadened mainly due to the Brownian motion (the average size of particles was < 200 nm and the angular dependence of the peak width was quadratic). In distilled water, ζ -potential of pyrite was negligible ($\zeta \approx 0$), while at pH 2 (10^{-2} N sulfuric acid) shifted to a negative value ($\zeta \approx -10$ mV) even though the proton concentration increased nearly 100,000-fold. Sulfate was considered to bound to pyrite. However, when 12.5 M Fe(III) sulfate was also added, ζ was less negative (again $\zeta \approx 0$) due to ferric ions bound to the pyrite-sulfate complexes. When pyrite was mixed and incubated for 5 min at the pH 2 ($\zeta \approx -10$ mV) with the pyrite-grown *T. ferrooxidans* (having a slightly positive ζ -potential due to the residual ferric ions in the cell wall, see the paragraph (ii)) a new broad ELS spectrum was obtained with the ζ -potential between those of pyrite and *T. ferrooxidans* alone, exhibiting the polydispersity of pyrite but the size of the bacterial cells (indicated by the linear angular dependence of the peak width). Apparently, fine pyrite particles were adhered to the cells due to the electrostatic attraction. No spectra have been shown for the mixture of (negatively charged) pyrite with the (also negatively charged) ferrous ions-grown *T. ferrooxidans*. Similar results were obtained for the mixture of stable particles of colloidal sulfur ($\zeta \approx -40$ mV) and slightly negative sulfur-grown *T. ferrooxidans*, incubated for 5 to 20 min).

The conclusion of the authors was that *T. ferrooxidans* under physiological conditions appears to regulate the net surface charge on its surface to minimize electrostatic (double layer) repulsive forces with the negatively charged solid substrates.

Ohmura et al. (1993a) studied the mechanism of microbial flotation using *T. ferrooxidans* ATCC 23270 for the pyrite suppression in the presence of 0.75 ml/l methyl isobutyl carbinol as a reagent. The particle concentration and size of pyrite was 20 g/l and 50-70 μm , respectively. They found that

(1) the flotation liquor containing *T. ferrooxidans* cells (cultured in the 9K basal salt medium, passed through a filter to remove precipitates of ferric compounds, centrifugated at 15,000 g for 15 min for collection, washed three times, and resuspended in an aqueous solution of sulfuric acid at pH 2) and no metabolic products suppressed the pyrite floatability most effectively. For example, at the bacterial density of 5.5×10^8 cells/ml and the bacterial contact time set at 10 min, the pyrite floatability decreased from 92 % (in a pH 2 aquatic solution control) to 32 %. The filtrate flotation liquor (centrifugation supernatant passed through a membrane filter with the pore size of 220 nm) alone, i.e. without the bacteria but with their extracellular components (metabolic products such as proteins or lipids), also manifested a slight suppressive effect (72 % pyrite floatability).

(2) the pyrite floatability decreased (exponentially) with the increasing total bacterial density in the flotation liquor to a fixed level with no significant change for at least 30 min (e.g. from ca. 57 % at 2.0×10^8 cells/ml to ca. 20 % at 12.0×10^8 cells/ml). Moreover, the pyrite floatability decreased linearly with the increase in cells adhering to the pyrite surface and at the total bacterial density above 2.0×10^8 cells/ml free (not adhered) cells were also present in the flotation liquor. The amount of the adhered cells to pyrite was estimated from the difference between the bacterial density of added and free cells, as measured visually by counting cells under a phase contrast microscope. A maximal suppression, i.e. a minimal pyrite floatability was observed for a total density of bacteria from which 4.5×10^8 cells/ml were adhered, representing up to 25 % coverage of the pyrite surface.

(3) There was no difference in the pyrite flotation suppression as well as the cell adhesion when bacteria with different iron-oxidizing ability (determined by the standard manometric method using the Warburg apparatus) were used. Even cells completely deactivated by suspending in 10 μM sodium cyanide for 10 min were able to suppress pyrite with an unchanged efficiency.

The above findings provided a clear explanation of the mechanism of the pyrite flotation

suppression as follows: bacterial cells in the flotation liquor adhere to the pyrite surface in a few seconds, changing its surface character from hydrophobic to hydrophilic; the suppression level depends on the number of adhered bacterial cells and it is not related to the surface oxidation by these cells.

In a 0.5 % sodium chloride solution, Ohmura et al. (1993b) observed a clear relationship between the hydrophobicity of four minerals, namely quartz, pyrite, galena, and chalcopyrite, and the number of cells of *Escherichia coli* HB101 adhered to them. The minerals were crushed into fine particles, sieved (200-300 mesh), washed with 5 ml of pH 2 sulfuric acid or a 0.5 % (wt/vol) sodium chloride solution several times to remove entrapped ultrafine particles, and suspended in a 1 % sodium chloride solution. The average size of the (very similar) distributions of the mineral particles ranged between 61.7 to 64.6 μm . The hydrophobicity was characterized on the mineral plates by the contact angle with a pH 2 sulfuric acid solution (28.4°, 68.9°, 80.9°, and 83.4°, respectively) or with a 0.5 % sodium chloride solution (32.5°, 76.3°, 94.3°, and 88.6°, respectively). The hydrophobicity of *E. coli* was evaluated by the contact angle ($\approx 31^\circ$) on a thin layer of the cells (cells were concentrated by centrifugation, spread on glass or acrylic plates, and dried at room temperature for 4 to 5 h) as well as by the BATH test in a biphasic system (0.1 to 0.5 ml of n-hexadecane mixed with 3 ml of a cell suspension + 0.5 % sodium chloride, stirred for 1 min, and separated for 5 min). It was concluded that *E. coli* tended to adhere to more hydrophobic minerals by hydrophobic interaction.

However, a lot of the *T. ferrooxidans* cells ATCC 23270 in the iron-free pH 2 sulfuric acid solution adhered to iron-containing minerals such as pyrite (25 % of added cells) and chalcopyrite (14 % of added cells) and only a few adhered to galena (1.4 %) and quartz (4.6 %) so that their adhesion could not be related to the hydrophobicity of the minerals. The ζ -potential of pyrite and *T. ferrooxidans* in the pH 2 sulfuric acid solution were -7.0 and -4.6 mV, respectively. Hence, despite the electrostatic repulsion *T. ferrooxidans* „recognizes“ the reduced iron in the mineral surfaces and selectively adhere to pyrite (and chalcopyrite) through a strong interaction other than the physical (hydrophobic) interaction.

The contact angles on a dry films of *T. ferrooxidans* with the pH 2 sulfuric acid solution were $22.7 \pm 1.9^\circ$ (glass plates) and $24.0 \pm 2.9^\circ$ (acrylic plates) and 75 % of the cells remained in the solution (BATH method) using 0.5 ml of n-hexadecane.

Takeuchi and Suzuki (1997) studied the effect of the potassium phosphate concentration (the normal buffer used for the sulfur oxidation studies) and pH on the hydrophobicity of *Thiobacillus thiooxidans* and its adhesion to solid elemental sulfur insoluble in water. The cells of *T. thiooxidans* ATCC 8085 were grown statically for 4 days in the Starkey's medium 1 adjusted to pH 2.3 with sulfuric acid, with elemental sulfur spread on the surface, collected at the end of the logarithmic phase after the removal of the sulfur by filtration, washed, and suspended in 50 mM potassium phosphate (pH 2.3).

With the increasing potassium phosphate concentration at pH 2.3, the cell surface hydrophobicity (evaluated from the portion of cells remaining in the aqueous phase by the BATH method using 3 ml-suspension of cells+3 ml of n-hexadecane) increased as follows: 88 % (1 mM), 78 % (50 mM), 37 % (0.1 M), 8 % (0.5 M), and 8 % (1.0 M). Ammonium sulfate had a similar effect as potassium phosphate. The addition of ethylene glycol counteracted the effect of a high potassium phosphate concentration (58 % at 0.5 M). The effect of the potassium phosphate concentration was similar at pH 7.5. The effect of pH at 50 mM potassium phosphate was not as dramatic (64 % at pH 2.3, 45 % at pH 5.0 to 5.5 and 58 % at pH 7.0 to 7.5).

Adhesion of *T. thiooxidans* onto sulfur was determined as follows: Cells (5 mg of wet weight in 10 ml of the buffer) were shaken in 50-ml flasks for 15 min at 200 rpm. The sulfur suspension (3.2 g per 10 ml with 500 rpm Tween 80) was added and the mixture was shaken for a further 15 min. The mixture was then filtered through a fluted filter paper and absorbance of the filtrate was measured at 660 nm and compared to that of the control without sulfur. At pH 2.3, nearly 70 % of the cells were adhered onto sulfur at 0.1 mM, 29 % at 10 mM, 22 % at 50 mM, and only 18 % at 0.1 M potassium phosphate so that the adhesion was not considered due to the hydrophobic interaction. Ammonium sulfate also inhibited the cell adhesion. The effect of pH at 50 mM potassium phosphate on the cell adhesion to sulfur was even less dramatic than its effect on the cell hydrophobicity. A slightly higher adhesion (≈ 40 % adhered cells) at pH 5.0 to 5.5 corresponded approximately to the pH range where the cell hydrophobicity was maximal (45 % of cell remained in the aqueous phase).

Solari et al. (1992) measured hydrophobic and electrokinetic properties of a (slightly hydrophobic) pure strain of *T. ferrooxidans* that were correlated with its adhesion to some sulphide (moderately hydrophobic) and quartz (hydrophilic) mineral surfaces. The cells of the *T. ferrooxidans* strain ATCC 1985 were grown in the basal medium MS9B at pH 2.5 with pills of elementary sulfur as the sole energy source. At the seventh day of incubation, they were centrifuged at 2000 rev min⁻¹ to separate out any sulfur particles. The supernatant was then again centrifuged at 10,000 rev min⁻¹ to

wash off the culture medium. The pellet of cells was washed and resuspended ($1-2 \times 10^9$ cells/ml) in the basal medium MSHCl (a salt solution similar to the MS9B medium but low in sulphate ions, containing 0.1 g/l NH_4Cl , 0.04 g/l $\text{K}_2\text{HPO}_4 \cdot 3\text{H}_2\text{O}$ and 0.1 g/l $\text{MgSO}_4 \cdot 7\text{H}_2\text{O}$) with the ionic strength 5×10^{-3} M. The flotation concentrates containing more than 95 % of pure sulphide minerals (chalcopyrite, pyrite, enargite, marcasite, chalcocite, covellite, and bornite) were sized (32 to 74 μm), deslimed with distilled water and cleaned for two h (leaching in 2 A sulphuric acid at 60 °C followed by repeated washing in distilled water, washing in acetone and drying in an oven at 30 °C) to decompose soluble impurities and flotation reagents. Quartz was first ground in a porcelain mill, purified by mild leaching in hot HCl (0.1 M, 2 h) until no dissolved iron was detected, and washed with distilled water until no trace of chloride was detected.

It has been observed that in the MSHCl medium the cells exhibited an isoelectric point (IEP) at pH 3.0. For minerals in the same medium pH_{IEP} was at about 2.2 (quartz) and 2.0 (chalcopyrite). Pyrite, however, had two IEP's at pH 4.5 and 5.7.

The liquid-liquid partition (BATH) test (5 ml of the cell suspension + 2 ml of hexadecane, 5 min of shaking and 5 min of standing) showed that the cells adhere weakly to hexadecane and that the adhesion increases at a lower pH due to the neutralization of ionized carboxylic groups in the fatty acid components of the outer cell wall. For example, the partition to hexadecane was 14.3 ± 0.8 % at pH 3.0 vs. 22.1 ± 3.6 % at pH 1.4. The contact angle of a drop of the MS9B medium on the fresh cell layer (collected on a 0.45 μm filter by vacuum filtering the cell suspension) at pH 3.0 was $20.3 \pm 4.2^\circ$. After 24 h drying the contact angle was $24.3 \pm 1.6^\circ$. With the MSHCl medium at pH 2.3, the contact angle was $23.3 \pm 2.4^\circ$. The surface free energy of the cells was calculated by the equation of state $67 \text{ mJ} \cdot \text{m}^{-2}$.

The liquid-liquid partition test showed that only quartz was hydrophilic (as its particles were wholly extracted in the aqueous phase), while chalcopyrite and pyrite were mildly hydrophobic (their particles were concentrated at the hexadecane/water interface) with the contact angle 66° .

The amount of 250 mg of the mineral particles was conditioned with 5 ml of the cell suspension in 20 ml test-tube in an incubator shaker at 200 rev min^{-1} (a most turbulent mixing procedure, denoted as C). The cell adhesion was calculated as the number of cells removed (20 μl) for periods up to 28 h from the solution over the mineral surface area (counted microscopically). Using the mixing procedure B (lowest turbulence), at pH 2.3 to 2.5 the equilibrium adhesion level for the sulphides (attained obviously after 5 h) was estimated in millions cells adhered per cm^2 as follows: 50 (chalcopyrite), 40 (pyrite), 55 (enargite), 25 (marcasite), 37 (chalcocite), 40 (covellite), and 30 (bornite). For quartz, using the mixing procedure A the equilibrium adhesion level (after 25 h) was higher at pH 1.4 (ca. 30×10^6 cells/ cm^2) than at pH 2.8 (ca. 17×10^6 cells/ cm^2). Generally, largest degree of the cell adhesion was obtained for chalcopyrite, followed by pyrite and quartz, with the surface coverage calculated using the above equilibrium adhesion levels to be 23.0, 20.0 and 9.8 %, respectively. The free energy of adhesion ΔG_{adh} , calculated according to the Volmer theory (from the equilibrium degree of the surface coverage and the volume fraction of the cell suspension) was -2.77 kT, -1.4 kT, and -1.66 kT, respectively. These small values of ΔG_{adh} are typical for a mechanism of adhesion occurring in the secondary minimum.

Knowing the fact that bacteria are sensitive to the nutritional requirements and starvation causes changes in the nature of their cell surface properties, Misra et al. (1996) studied the effect of the culture medium of *T. ferrooxidans* on its pyrite depression. Three culture media with different nutrient composition were used for the growth of the bacterium: 9K Standard Medium (SM), Phosphate Deficient Medium (PDM), and Pyrite Added Medium (PAM). The 4-day old bacterial culture was first passed through a Whatman filter paper No. 44 to remove the precipitates. The filtrate was then centrifuged at 15,000 rpm for 30 min. The residual cell pellet was suspended in a solution of sulfuric acid at pH 1.8 and allowed to stand for 2 h to permit settling of any precipitates. The supernatant with cells was again centrifuged as described above until no iron was present so that iron-free cell suspensions were used.

The contact angle of a water drop on a polished pyrite surface decreased as the concentration of the cell suspensions increased (the pyrite was conditioned with the cell suspensions on a rotary shaker at pH 2.3 for 30 min, removed and dried). For example, without the addition of the cells, the contact angle of pyrite was 49° but with the SM-grown cells adhered (at the concentration of 1.9×10^8 cells/ml) on it the contact angle decreased to 23° . The PDM-grown cells gave lower values of the contact angle. The pH_{IEP} of the cells also varied depending on the culture medium used. In the presence of 5×10^{-4} M NaCl, the SM-, PDM-, and PAM-grown cells had the values 2.0, 3.2, and 3.7, respectively. In adhesion experiments, 100 mg of pyrite (53-74 μm) was washed with sulfuric acid (pH 1) for 10 min and mixed with 50 ml of the cell suspension (10^8 cells/ml) at pH 2. The suspension was stirred for the period of 30 min and allowed to settle. The supernatant was withdrawn to determine the

concentration of cells. The amount of the cells adhered on pyrite was determined by the difference in the cell concentration before and after the addition of pyrite. The adhesion of the SM-, PDM-, and PAM-grown cells was found to be ca. 1.8×10^5 , 3.5×10^5 , and 4.2×10^5 cell/mg pyrite, respectively. The increased capacity of the phosphate-starved cells to attach themselves to the pyrite surface was found to be related to changes in the outer membrane proteins (an increase in the high molecular weight fraction) and a 25 % increase in the lipopolisaccharides (in comparison to the SM-grown cells). The optimized pyrite flotation was carried out at pH 9.0 using a combined biotreatment with the cells (at pH 1.8) and purified sodium isopropylxanthate (1.6×10^{-4} M, pH 9.0) as a collector. Again, the pyrite flotation recovery decreased in the same order, i.e. ca. 70 %, 30 %, and 10 % for the SM-grown, PDM-grown, and PAM-grown cells, respectively. The increase of pH of the bacterial conditioning with the PAM-grown cells (flotation with the xanthate was still at pH 9.0) resulted in a decrease in the recovery from ca. 43 % (pH 1.2) to 15 % (pH 6.5).

Mineral surface characteristics

The study of the surface properties of sulfides is complicated by changes in the surface layer structure and composition due to chemical interactions with water and oxygen. On the sulfide surface, different compounds such as hydroxides, sulfates, thiosulfates or elemental sulfur can be formed. The high scatter in published values of the pH_{IEP} and zeta potentials can be ascribed to the poor control of the experimental (pretreatment) conditions and to the solubility of sulfides.

Durán et al. (1994) estimated the LW and AB surface free energy components of highly pure (synthetic), colloidal particles of zinc sulfide (sphalerite homogeneous in size of 320 ± 20 nm and spherical shape), as well as of commercial ZnS both unoxidized and oxidized by hydrogen peroxide (2 g of ZnS suspended in 35 ml of 3 % and 15 % aqueous H_2O_2 solution for 1 h and cleaned by centrifugation and redispersion in distilled water), ZnO and $ZnSO_4 \cdot H_2O$. To estimate the above components, contact angles were measured on pellets obtained by compressing a dry powder under 10^9 Pa for 10 min, drying at $105^\circ C$, and kept in a dessicator („dry“ pellets) or saturated with water vapor at room temperature („wet“ pellets). The water contact angle measured was as follows: 40° (commercial ZnS), 37° (3 % H_2O_2 -treated commercial ZnS), 45° (15 % H_2O_2 -treated commercial ZnS), 32° (ZnO), and 15° ($ZnSO_4 \cdot H_2O$). The thin-layer wicking technique was also used. In this technique, a homogeneous thin layer of particles was laid on microscope glass slides by spreading 2 ml of the 50 g/l suspension and drying for 24 h at room temperature and then oven-dried at $60^\circ C$ for 6 h and stored in a dessicator („bare“ plates) or contacted for several hours with the vapor of the liquid to be used („preconcentrated“ plates).

From the contact angle measurements (with the water-formamide-diiodomethane triade on the dry pellets), the γ_S^{LW} component was determined to be ≈ 48 mJ/m² for all powders. A comparable value was determined for synthetic ZnS (52.4 ± 4 mJ/m²) and commercial ZnS (45.0 ± 4 mJ/m²) by the thin-layer wicking technique. Concerning the γ_S^+ component it was ≤ 1 mJ/m² with no significant differences between dry and wet pellets of all powders including ZnO and $ZnSO_4 \cdot H_2O$. Hence, all the powders are strong electron donors (as confirmed also by the thin-layer wicking technique). Really, the γ_S^- component was 38.0 mJ/m² (commercial ZnS), 39.5 mJ/m² (3 % H_2O_2 -treated commercial ZnS), 35.3 mJ/m² (15 % H_2O_2 -treated commercial ZnS), 43.4 mJ/m² (ZnO), and 52.8 mJ/m² ($ZnSO_4 \cdot H_2O$). The thin-layer wicking however gave the γ_S^- component of synthetic ZnS higher (≈ 88 mJ/m²) than that of other powders (e.g. 54.7 mJ/m² for commercial ZnS).

In order to complete the characterization of the above ZnS samples, electrophoretic mobility was measured as a function of both the concentration of potential-determining ions (Zn^{2+} and S^{2-}) and the oxidation extent (Durán et al., 1995). The samples were cleaned by repeated cycles of centrifugation and redispersion (50 mg/l) in deoxygenated water at pH 5.5 and kept in the dark under N_2 atmosphere until the determinations were carried out. It has been found that the pH_{IEP} of the colloidal ZnS is 5.3 in the presence of 10 mM KNO_3 . It is shifted to the value of ca. 10 when 10 mM $Zn(NO_3)_2$ is added due to the specific adsorption of Zn^{2+} on the colloid. More specifically, the precipitated $Zn(OH)_2$ has been expected to be present on the surface. It has also been shown that the pH_{IEP} of the commercial ZnS (ca. 4) was shifted after oxidation (ca. 5 and 7 for the 3 % and 15 % H_2O_2 -oxidized ZnS, respectively) as a consequence of the formation of $Zn_2(OH)_2SO_4(s)$ or $Zn(OH)_2(s)$ on the ZnS surface containing originally primarily S^0 . The pH_{IEP} of ZnO was ca. 9.5.

Good et al. (1993) set out to determine both the liquid-advancing (θ_a) and liquid-retreating (θ_r) angles (a measure of the surface energy of the lower-energy and higher-energy patches or areas, respectively) by the captive sessile drop technique and to correlate them with the surface composition (i.e. rank) of selected coals and two graphites determined by ESCA. Coal samples were from a total of 15 different sources: two anthracites, one semianthracite, 10 bituminous (of ranks from LV to HVC),

one sub-bituminous and one lignite. The samples were cleaved or sawed parallel to bedding planes, ground flat with a fine grade emery paper, and polished using 0.05 μm alumina, under nitrogen.

A correlation was found when the water contact angle vs. surface atom % carbon (an uptrend above $\approx 76\%$ C) and vs. surface % oxygen (an uptrend below $\approx 18\%$ O) was plotted. In both cases the uptrend started from $\theta_{\text{Wa}} \approx 75^\circ$ and $\theta_{\text{Wr}} \approx 15^\circ$ and was steeper for the set of samples that were prepared and measured in nitrogen than those in air. The electron-donor surface energy component for the higher-energy areas, γ_{Sr}^- , decreased from near 40 mJ/m^2 (low-rank coal, e.g. lignite and some bituminous coals) to near 20 mJ/m^2 (anthracite and graphite). The electron-donor surface energy component for the lower-energy areas, γ_{Sa}^- , also decreased from near 9 mJ/m^2 (low-rank coals) to 1 mJ/m^2 (graphite). By contrast, the electron-acceptor surface energy component was approximately independent of coal rank ($\gamma_{\text{Sr}}^+ \approx 1.8 \text{ mJ/m}^2$, $\gamma_{\text{Sa}}^+ \approx 0.2 \text{ mJ/m}^2$) as was also the apolar Lifshitz-van der Waals surface energy component ($\gamma_{\text{Sr}}^{\text{LW}} \approx 49.7 \text{ mJ/m}^2$, $\gamma_{\text{Sa}}^{\text{LW}} \approx 39.7 \text{ mJ/m}^2$). The latter values are compatible with the estimate for the γ_{c} of coal (independent of rank) 46.5 mJ/m^2 .

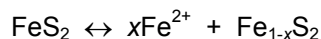
Coal is a very heterogeneous substance so that the mechanism of the surface charge generation is very complex. In general, when a freshly fractured coal surface is exposed to the atmosphere, the exposed carbon atoms in the lattice react with atmospheric oxygen (natural weathering). Oxidation can be also due to deliberate contact with oxidants, e.g. hydrogen peroxide (artificial weathering). Lignites (low-rank coals subjected to the least amount of metamorphic change during the coal-forming process) are characteristic by their high oxygen and moisture contents and less carbon than higher rank coals such as bituminous and anthracite. Oxygen is present in a variety of surface functional groups. Hence, the surface charge of low-rank lignitic coals is specifically determined mainly by the degree of dissociation of weakly acidic oxygen-containing functional groups such as phenolic OH and carboxylic COOH (in the first instance the coal surface can be considered as containing only carboxylic groups). At high pH the surface carboxyls will tend to dissociate and the surface acquires a strong negative charge, while at low pH they will be protonated and the surface charge diminishes. At a very low pH the surface may even become positively charged.

Oxidation, whether it be natural or artificial proceeds in three stages: Stage I is superficial oxidation characterized by the formation of acidic coal-oxygen complexes (surface functional groups, see above); In the Stage II, organic components of coal form alkaline-soluble hydroxy carboxylic acids with various molecular weights (humic acids) which then degrade to simple water-soluble acids (Stage III). To evaluate the surface oxidation of coals, electrokinetic measurements can be used (Quast and Readett (1987). For example, it is known that the pH_{IEP} of a high volatile A bituminous vitrain decreases with oxidation from 4.5 (unoxidized) to 3.4 (oxidation with pure oxygen for 24 h at 125°C) and no pH_{IEP} is measurable after oxidizing for 120 h or more. Also, the variations in the electrophoretic mobility due to oxidation are relatively small in magnitude at $\text{pH} > 7$ when compared to variations at $\text{pH} < 7$. This can be attributed to the solubility of humic acids (the surface of vitrain oxidized for 380 h was completely converted to humic acids). The pH_{IEP} of a high volatile bituminous coal can even drop from 5 to 1.2 after oxidation with H_2O_2 for 4 h at 80°C. Or, the pH_{IEP} of a coal is 1.6 (weathered surface coal with the oxygen content of 17.61 %) compared to 4.1 (unweathered coal found at a depth of about 50 m with $< 5\%$ O). Therefore, oxidation causes the electrophoretic mobility of high rank coals to become more negative (especially at in the acidic medium) as a result of an increase in carboxylic and phenolic surface functional groups (benzene rings containing electron-donating groups are much weaker acids). Similarly, the surface of lignites is negatively charged except under strongly acidic conditions ($\text{pH} \leq 2$) where acidic functional groups are ionized.

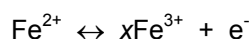
Oxidation, of pyrite results in an inevitable modification of the solution as well as of its surface properties. The final stage of this oxidation is an oxide or hydroxide film at the pyrite surface in the form of goethite, magnetite or hematite. However, several mechanisms have been proposed for the early stage of oxidation with adsorption of dissolved molecular oxygen or water molecules at the pyrite surface and the formation of various intermediates such as ferrous, ferric, sulphite and sulphate ions, sulphur and ferric hydroxide that change the electrokinetics and hydrophobicity of the surface appreciably (Fornasiero et al., 1992). The latter authors studied the oxidation of pyrite by measuring its electrophoretic mobility as a function of pH under various pretreatment conditions. It has been found that the negative pyrite surface becomes less negatively or even positively charged when the time of conditioning increases. In other words, the pH_{IEP} was shifted to higher values (close to the pH_{IEP} of ferric hydroxide). For example, at the conditioning pH 5, the pH_{IEP} was about 1.2 (pretreated for 0.5 h in argon), 3 (0.5 h in air), 4.8 (2 in air), and 6 (19 h in air). Hence, the change was very fast in the first 2 h but slowed down for longer conditioning times and the pH_{IEP} 1.2 obtained under an argon atmosphere was adopted to represent the „virgin“ pyrite surface. Pyrite is thus strongly acidic sulfide. The conditioning gas also influenced the surface charge. For example, the pH_{IEP} was about 6.8 in oxygen (for conditioning pH and time of 0.5 h and 5, respectively). This indicated that dissolved oxygen

is involved in the decrease of the magnitude of the zeta potential and the reversal of its sign. Concerning the conditioning pH, no or little change in the electrical properties of pyrite occurred at conditioning pH values ≥ 7 , despite the presence of oxygen in the system.

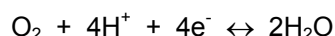
Pyrite oxidation was proposed to proceed through three steps: Step I is dissolution of ferrous ions and formation of an iron-deficient, sulphur-rich surface rather than elemental sulphur:



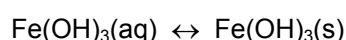
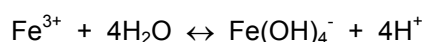
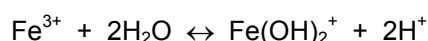
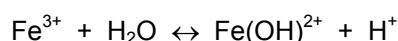
Stage II is oxidation of ferrous ions to ferric ions at positive oxidation potentials (anodic reaction):



Whereas the cathodic reaction involves dissolved molecular oxygen:



Stage III is hydrolysis of ferric ions to ferric hydroxo-complexes, whose concentrations are also pH-dependent, namely:



The solid ferric hydroxide produced in the last reaction decomposes slowly to thermodynamically more stable forms, i.e. goethite, magnetite and hematite. Therefore, the dependence of the zeta potential of pyrite on pH in various pretreatment conditions can be explained by the pH-dependence of the concentration of Fe^{3+} and O_2 (Stage II) as well as the pH-dependent specific adsorption of positively charged hydrolysed ferric ions (especially $\text{Fe}(\text{OH})^{2+}$ and $\text{Fe}(\text{OH})_2^+$) onto the pyrite surface (Stage III).

Summarization

From the above summarized results follows:

(1) *T. ferrooxidans* cell wall

The surface charge of *T. ferrooxidans* is obviously very low at physiological conditions (pH about 2) and depends on the presence of residual ferric ions in the cell wall (these ions may originate in the 9K liquid growth medium or by dissolution of pyrite as a solid substrate). In fact, the pyrite-grown cells have the zeta potential less negative (or more positive) (pH_{IEP} close to 3.7) than that of the 9K medium-grown cells (pH_{IEP} close to 2). Having the water contact angle $\theta_{\text{W}} \approx 23^\circ$, the cells can be considered as hydrophilic or slightly hydrophobic. No determinations have been conducted in order to evaluate their surface energy components.

(2) Minerals and coal surface

In general, the native surfaces of most sulfides are acidic in character with the pH_{IEP} from 2 to 3. However, they are to a different degree susceptible to oxidation (i.e. conditioning pretreatment). Pyrite is also an acidic sulfide mineral, strongly liable to oxidation. When unoxidized, its only pH_{IEP} is close to 1.2. Oxidation by air is very fast during first two hours, causing a dramatic increase in the pH_{IEP} to the value of 4.8 and two pH_{IEP} values are typically found. Most electrokinetic studies of (oxidized) pyrite report the values of pH_{IEP} about 6 or more.

Both surface energy components and the surface charge have been determined for only one sulfide, viz. ZnS (sphalerite). Its γ_{S}^- as well as pH_{IEP} increased with oxidation: respectively, 40 mJ/m^2

and 4.0 (for commercial sphalerite) vs. 88 mJ/m² and 5.3 (for synthetic, partially oxidized sphalerite). Oxidation however did not change γ_{S^+} (≤ 1 mJ/m²) nor $\gamma_{S^{LW}}$ (about 50 mJ/m²).

On the other hand, aside from oxidation and the complications due to the surface and phase heterogeneity and high porosity, the surface energy and electrokinetics of the coal surface is well defined. Unoxidized high-rank coals (anthracite) are characteristic by a relatively basic surface (γ_{Sr^-} is typically 20 mJ/m², γ_{Sa^-} 1 mJ/m² and pH_{IEP} is close to 5) while oxidation causes an acidification. So, low-rank coals (e.g. lignite or some bituminous coals) have γ_{Sr^-} about 40 mJ/m², γ_{Sa^-} 9 mJ/m² and pH_{IEP} is close to 2. For strongly oxidized (acidic) coals no pH_{IEP} is observed. By contrast, γ_{Sr^+} and γ_{Sa^+} is independent of the coal rank (about 1.8 and 0.2 mJ/m², respectively). The same case is with $\gamma_{Sr^{LW}}$ and $\gamma_{Sa^{LW}}$ (about 50 and 40 mJ/m², respectively).

(3) Adhesion of *T. ferrooxidans* on mineral and coal surface

At pH close to 2, the cells of *T. ferrooxidans* (with slightly positive or negative surface charge) may adhere on unoxidized ($\zeta \approx -10$ mV) as well as on oxidized ($pH_{IEP} = 4.5$) pyrite. Furthermore, adhesion was observed between the sulphur-grown (slightly negative) cells of *T. ferrooxidans* and sulphur ($\zeta \approx -40$ mV). *T. ferrooxidans* (with $\zeta = -4.6$ mV) may also adhere to other acidic sulphides such as chalcopyrite but not on quartz or galena.

Applicability of the model

It can be concluded that there are only few complementary measurements on the electrokinetics and the surface energy components of minerals and coals. Moreover, the surface energy components are even unknown for *T. ferrooxidans* and the most important sulfides, including pyrite. That is why it is not possible yet to decide if the colloidal model of microbial adhesion is feasible to predict the initial stage of the attachment of *Thiobacilli* onto mineral surfaces. However, the free energy of interaction between a fictive hydrophilic bacterial cell such as *T. ferrooxidans* and some sur-

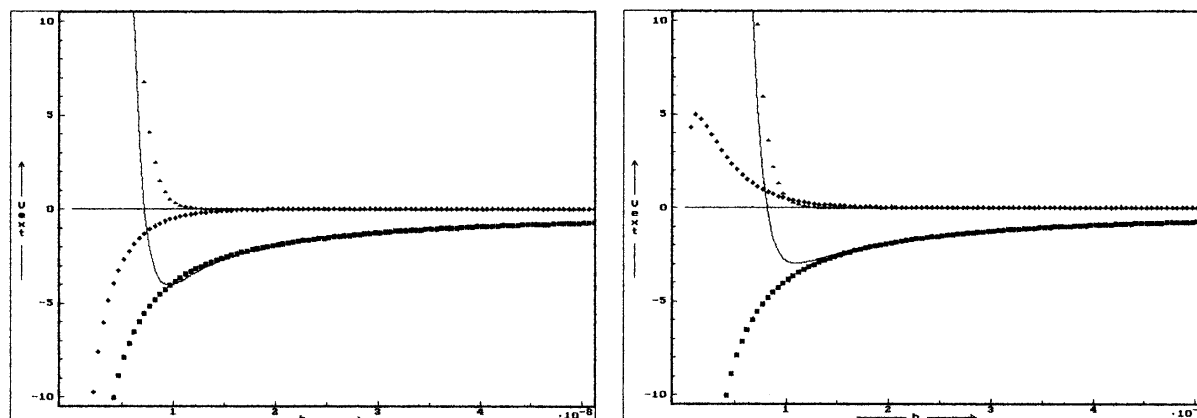


Fig. 1. Free energy of interaction of a fictive hydrophilic bacterium (extended DLVO model, V_{ext} , in kT units) as a function of the separation (h , in nm) from higher-energy patches of an unoxidized (a) and oxidized (b) coal surface (substrate) in water at pH 2. Model parameters for the bacterium: $a = 1 \mu m$, $\gamma_b^{LW} = 35$ mJ/m², $\gamma_b^+ = 0.6$ mJ/m², $\gamma_b^- = 60$ mJ/m², $\zeta_b = -5$ mV. Model parameters for coal: $\gamma_s^{LW} = 50$ mJ/m², $\gamma_s^+ = 1.8$ mJ/m², $\gamma_s^- = 20$ mJ/m² (a) and 40 mJ/m² (b) (data from Good et al., 1993), $\zeta_s = +10$ mV (a) and -10 mV (b). Curves represent the van der Waals (■), electrostatic (◆), structural (▲), and total (—) component of the free energy of interaction. For more details about the model see Škvarla (1993).

faces whose model parameters are known, namely higher-energy and lower-energy patches of an unoxidized and oxidized coal (Fig.1 and 2), quartz (Fig.3) and sphalerite (Fig.4) has been calculated as a function of the surface separation for illustration. Two interesting features can be observed using the model with the data. First, the bacterial attachment on both minerals (quartz and sphalerite) as well as coal, except the lower-energy patches of unoxidized coal attracting the cells at all surface separations, may occur in the so-called secondary minimum. This means that the bacterial attachment would be of the reversible character. Second, as already mentioned, the (irreversible) attachment of the bacterium on the lower-energy patches of unoxidized coal is supposed to occur in the so-called primary minimum. Unfortunately, due to the absence of proper parameters, the model cannot explain the selective adhesion of *T. ferrooxidans* onto pyritic surface.

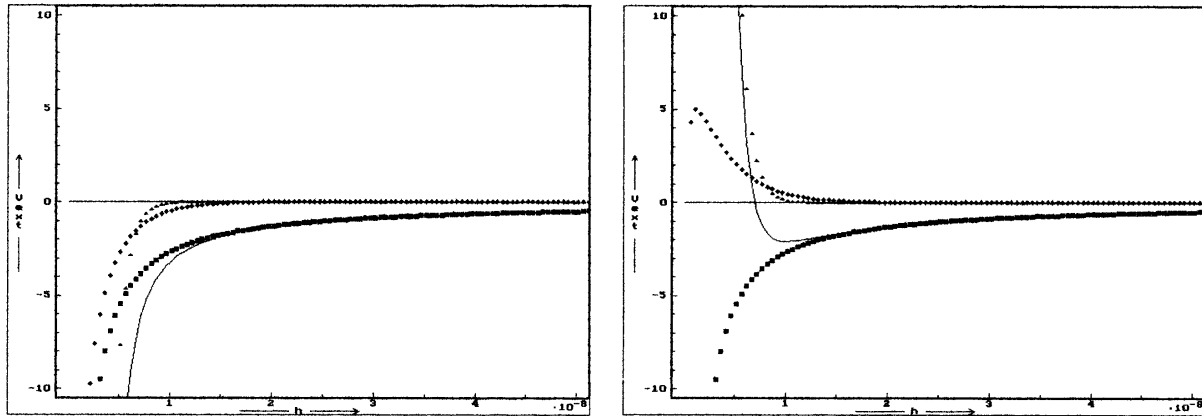


Fig.2. Free energy of interaction of a fictive hydrophilic bacterium (extended DLVO model, V_{ext} in kT units) as a function of the separation (h , in nm) from lower-energy patches of an unoxidized (a) and oxidized (b) coal surface (substrate) in water at pH 2. Model parameters for the bacterium: $a = 1\mu\text{m}$, $\gamma_b^{LW} = 35\text{ mJ/m}^2$, $\gamma_b^+ = 0.6\text{ mJ/m}^2$, $\gamma_b^- = 60\text{ mJ/m}^2$, $\zeta_b = -5\text{ mV}$. Model parameters for coal: $\gamma_s^{LW} = 40\text{ mJ/m}^2$, $\gamma_s^+ = 0.2\text{ mJ/m}^2$, $\gamma_s^- = 1\text{ mJ/m}^2$ (a) and 9 mJ/m^2 (b) (data from Good et al., 1993), $\zeta_s = +10\text{ mV}$ (a) and -10 mV (b). Curves represent the van der Waals (■), electrostatic (◆), structural (▲), and total (—) component of the free energy of interaction.

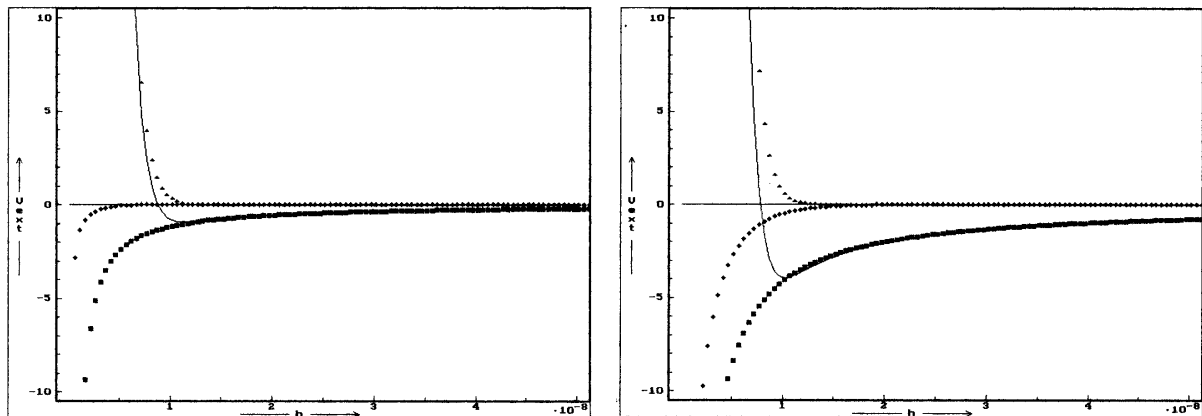


Fig.3. Free energy of interaction of a fictive hydrophilic bacterium (extended DLVO model, V_{ext} in kT units) as a function of the separation (h , in nm) from the quartz surface (substrate) in water at pH 2. Model parameters for the bacterium: $a = 1\mu\text{m}$, $\gamma_b^{LW} = 35\text{ mJ/m}^2$, $\gamma_b^+ = 0.6\text{ mJ/m}^2$, $\gamma_b^- = 60\text{ mJ/m}^2$, $\zeta_b = -5\text{ mV}$. Model parameters for quartz: $\gamma_s^{LW} = 29.1\text{ mJ/m}^2$, $\gamma_s^+ = 0.2\text{ mJ/m}^2$, $\gamma_s^- = 31.6\text{ mJ/m}^2$ (data for ground glass from Giese et al., 1993), $\zeta_s = 0$. Curves represent the van der Waals (■), electrostatic (◆), structural (▲), and total (—) component of the free energy of interaction.

Fig.4. Free energy of interaction of a fictive hydrophilic bacterium (extended DLVO model, V_{ext} in kT units) as a function of the separation (h , in nm) from the sphalerite surface (substrate) in water at pH 2. Model parameters for the bacterium: $a = 1\mu\text{m}$, $\gamma_b^{LW} = 35\text{ mJ/m}^2$, $\gamma_b^+ = 0.6\text{ mJ/m}^2$, $\gamma_b^- = 60\text{ mJ/m}^2$, $\zeta_b = -5\text{ mV}$. Model parameters for sphalerite: $\gamma_s^{LW} = 52.0\text{ mJ/m}^2$, $\gamma_s^+ = 0.7\text{ mJ/m}^2$, $\gamma_s^- = 68.6\text{ mJ/m}^2$ (data from Durán et al., 1995), $\zeta_s = +10\text{ mV}$. Curves represent the van der Waals (■), electrostatic (◆), structural (▲), and total (—) component of the free energy of interaction.

References

- Attia, Y.A., Elzaky, M., and Ismail, M.: Enhanced separation of pyrite from oxidized coal by froth flotation using biosurface modification. *Int. J. Miner. Process.*, **37**, 1993, p. 61-71.
- Blake II, R.C., Shute, E.A., and Howard, G.T.: Solubilization of minerals by bacteria: electrophoretic mobility of *Thiobacillus ferrooxidans* in the presence of iron, pyrite, and sulfur. *Appl. Environ. Micro-biol.*, **60**, 1994, p. 3349-3357.
- Durán, J.D.G., Delgado, A.V., González-Caballero, F., and Chibowski, E.: Surface free energy components of monodisperse zinc sulfide. *Mater. Chem. Phys.*, **38**, 1994, p. 42-49.
- Durán, J.D.G., Guindo, M.C., and Delgado, A.V.: Electrophoretic properties of colloidal dispersions of monodisperse zinc sulfide: Effects of potential-determining ions and surface oxidation. *J. Colloid Interface Sci.*, **173**, 1995, p. 436-442.

- Durán, J.D.G., Guindo, M.C., Delgado, A.V., and González-Caballero, F.: Stability of monodisperse zinc sulfide colloidal dispersions. *Langmuir*, 11, 1995, p. 3648-3655.
- Fornasiero, D., Eijt, V., and Ralston, J.: An electrokinetic study of pyrite. *Colloids Surfaces*, 62, 1992, p. 63-73.
- Giese, R.F., Wu, W., and van Oss, C.J.: Surface and electrokinetic properties of clays and other mineral particles, untreated and treated with organic or inorganic cations. *J. Disper. Sci. Technol.*, 17, 1996, p. 527-547.
- Good, R.J., Gardella, J.A., Huang, H. T-L., Weitzsacker, C., Islam, M., and Badgugar, M.: Variation of the surface composition of coal with rank, and its influence on the hydrophobic/hydrophilic properties of coal and graphite. *manuscript*, 1993.
- Misra, M., Bukka, K., and Chen, S.: The effect of growth medium of *Thiobacillus ferrooxidans* on pyrite flotation. *Miner. Eng.*, 9, 1996, p. 157-168.
- Ohmura, N., Kitamura, K., and Saiki, H.: Mechanism of microbial flotation using *Thiobacillus ferrooxidans* for pyrite suppression. *Biotechnol. Bioeng.*, 41, 1993a, p. 671-676.
- Ohmura, N., Kitamura, K., and Saiki, H.: Selective adhesion of *Thiobacillus ferrooxidans* to pyrite. *Appl. Environ. Microbiol.*, 59, 1993b, p. 4044-4050.
- Ohmura, N. and Saiki, H.: Desulfurization of coal by microbial column flotation. *Biotechnol. Bioeng.*, 44, 1994, p. 125-131.
- Ohmura, N. and Saiki, H.: Desulfurization of Pittsburg coal by microbial column flotation. *Appl. Biochem. Biotech.*, 61, 1996, p. 339-349.
- Solari, J.A., Huerta, G., Escobar, B., Vargas, T., Badilla-Ohlbaum, and Rubio, J.: Interfacial phenomena affecting the adhesion of *Thiobacillus ferrooxidans* to sulphide mineral surfaces. *Colloids Surfaces*, 69, 1992, p. 159-166.
- Škvarla, J.: A physico-chemical model of microbial adhesion. *J. Chem. Soc. Faraday Trans. (UK)*, 89, 1993, p. 2913-2921.
- Takeuchi, T.L., and Suzuki, I.: Cell hydrophobicity and sulfur adhesion of *Thiobacillus thiooxidans*, *Appl. Environ. Microbiol.*, 1997, 63, p. 2058-2061.